Journal of Food Engineering 119 (2013) 552–560

Contents lists available at SciVerse ScienceDirect

Journal of Food Engineering

journal homepage: www.elsevier.com/locate/jfoodeng

Using mobile metallic temperature sensors in continuous microwave assisted sterilization (MATS) systems

Donglei Luan [a], Juming Tang [a,*], Patrick D. Pedrow [b], Frank Liu [a], Zhongwei Tang [a]

[a] Department of Biological Systems Engineering, Washington State University, P.O. Box-646120, Pullman, WA 99164-6120, USA
[b] School of Electrical Engineering and Computer Science, Washington State University, P.O. Box-642752, Pullman, WA 99164-2752, USA

ARTICLE INFO

Article history:
Received 3 February 2013
Received in revised form 30 May 2013
Accepted 8 June 2013
Available online 20 June 2013

Keywords:
Electric field singularity
Heating pattern
Mobile metallic temperature sensor
Microwave heating
Temperature profile

ABSTRACT

The goal of this study was to evaluate suitability of using mobile metallic temperature sensors in continuous microwave assisted sterilization (MATS) systems. A computer simulation model using the finite difference time domain method was developed to study the influence of microwave field on the accuracy of mobile metallic temperature sensors, ELLAB, in a MATS system in which food packages with embedded sensors traveled on a conveyor belt. Simulation results indicated that the metallic temperature sensors did not change the overall heating patterns within food samples. But when a metallic temperature sensor was placed in parallel to the electric field component within microwave cavities the field intensity had intense singularity at the sensor tip and caused localized overheating. The electric field singularity adjacent to the tip of the metallic temperature sensor can be avoided by placing the sensor perpendicular to the electric field component. The simulated heating patterns and temperature profiles were verified with experimental results. It was evident from both simulated and experimental results that the metallic temperature sensor could be used to capture temperature profile in a MATS system when placed in a suitable orientation.

1. Introduction

Microwaves generate heat through interaction between dielectric materials, such as foods, and alternating electromagnetic (EM) fields. Compared with conventional water or steam heating, microwave volumetric heating has significant advantages in reducing process time and improving food quality (Guan et al., 2002, 2003). A single mode 915 MHz microwave assisted thermal sterilization (MATS) system was developed at Washington State University (Pullman, WA) to explore the use of the microwave technology in pasteurization and sterilization applications and collect engineering data for industrial scale-up (Tang et al., 2006). It is a 22 m long pilot-scale system that includes four sections: preheating, microwave heating, holding and cooling to simulate continuous industrial processes. Packaged food products are transported continuously through these four sections by a microwave transparent conveyor belt. Microwave heating section is the key part which can elevate the temperature of a food product by more than 50 °C (e.g., from 70 °C to 121 °C) in three minutes. This section has four connected single-mode microwave heating cavities each with a minor different internal configuration to provide complementary electric field distribution leading to a relative uniform final heating in foods after moving through those cavities at a constant speed.

Knowledge of heating pattern in foods and reliable measurement of temperature histories at desired locations are critical in developing a thermal process for production of safe foods. Heating pattern describes the temperature distribution within foods. It is used to evaluate heating uniformity and identify locations of least processed parts within food packages. The temperature profile records the changes in food temperature over processing time to provide data for calculations of projected reduction in targeted food pathogen population or possible thermal degradation of food qualities (Holdsworth, 1985). Temperature profiles are directly measured by temperature sensors at different locations within foods. In conventional thermal processing, the location that gains least heat and shows lowest temperature is called the cold spot. In microwave heating, the temperature distributions at different locations are caused by uneven electric field distributions. More than one cold spots may exist in a microwave heated food product. Likewise, hot spots may also be present at different positions in microwave heated foods. Unlike multi-mode microwave heating systems in which heating patterns are difficult to predict due to the co-existence of several resonant modes within the frequency bandwidth that coincides with the power spectrum of industrial microwave generators (Chan and Reader, 2000), the single mode MATS system can provide a stable and predictable heating pattern

* Corresponding author. Tel.: +1 509 335 2140; fax: +1 50 335 2722.
E-mail address: jtang@wsu.edu (J. Tang).

0260-8774/$ - see front matter © 2013 Elsevier Ltd. All rights reserved.
http://dx.doi.org/10.1016/j.jfoodeng.2013.06.003

(Resurrection et al., 2013). This was verified with an effective method that assesses the heating patterns based on formation of chemical marker (M-2) in model foods during microwave heating (Pandit et al., 2006, 2007a, 2007b; Resurrection et al., 2013).

Once the heating pattern and cold spots are determined, temperature sensors can then be directly placed at the locations of cold spots to record temperature profiles for developing a thermal process to ensure food safety. Fiber-optic thermometers are the most reliable and accurate means for direct temperature measurements in microwave heating because those sensors do not disturb microwave fields (Kyuma et al., 1982; Wang et al., 2003). In general, thermocouples and other metallic probes are not desirable for accurate temperature measurements in microwave environments due to possible strong interactions between metal parts and microwave fields (Datta et al., 2001). Strong microwave fields can cause electrical discharges and signal perturbations in metallic probes. Furthermore, the microwave fields are also distorted by the presence of metallic probes. In a previous study, to explore the use of thermocouples in microwave environments a thermocouple was shielded with an aluminum tube and grounded to the metallic wall to reduce electrical discharges and signal perturbations (Van De Voort et al., 1987). Ramaswamy et al. (1998) also reported effectiveness of several shielding constructions. Reasonably accurate results were obtained through proper designs (shield isolation and body insulation) of the shielding. However, in continuous microwave heating systems, neither the fiber-optic thermometers nor shielded thermocouples are applicable because of the need to connect those sensors to signal conditioning and data acquisition units that only operate in an open ambient environment outside microwave systems. Possible alternatives are mobile (wireless) temperature sensors, such as Tracksense Pro data logger (Ellab Inc., Centennial, CO, USA) and NanoVACQ temperature data logger (TMI-USA Inc., Reston, VA, USA) developed for temperature measurements in continuous conventional thermal processes. In operation, mobile temperature sensors imbedded in packaged foods collect and store temperature data during thermal processes. Afterward, those sensors are removed from food packages, and data downloaded into computers for analyses. A common mobile temperature sensor consists of two units: a probe for sensing temperatures and a base for storing temperature data (Fig. 2). The surfaces of both units are made of a metal sheet used for protecting the inner sensing and data storing elements. In microwave application, the surface protection can act as a shield to microwave energy based on the same principle as for shielded thermocouples reported in previous mentioned two studies. But the metallic shielding may also create disturbances to microwave field distribution and affect the heating pattern.

In studies of diffraction problems in EM fields, it has been found that the EM field components at sharp edges of diffracting obstacle may runway to infinity. This irregular sharp increase in EM field intensity is known as a singularity (Bouwkamp, 1946). The EM fields may have singularities at the vicinities of metal-dielectric wedges (Meixner, 1972; Bladel, 1985). Egorov et al. (2006) studied the edge effect in microwave heating of conductive plates. It was reported that the overheating in the edge vicinity of thin conducting plates was attributed to the diffraction of EM waves rather than the uneven irradiations. No studies have been reported to investigate the behavior of microwave fields diffracted by mobile metallic temperature sensors. Performance of the mobile metallic temperature sensor influenced by the diffracted EM field is also unknown. In this study we developed a computer simulation model to investigate the interaction between mobile metallic temperature sensors and microwave fields in MATS systems.

With the development of powerful computer workstation and professional software, computer simulation has been effectively used to numerically solve microwave heating problems based on different numerical methods. The finite-difference time-domain (FDTD) method is popular in solving coupled EM and heat transfer problems in microwave heating due to less computer memory and simulation time consumptions (Dev et al., 2010; Watanabe et al., 2010). Furthermore, arbitrarily shaped geometries can be simulated after the conformal FDTD method was developed (Holland, 1993). Chen et al. (2007, 2008) developed simulation models for food packages processed in continuously moving microwave heating system based on conformal FDTD method. The system contained two microwave heating cavities which were similar to the cavities in MATS system. Resurrection et al. (2013) developed a computer simulation model (CSM) for MATS systems based on the dimension of the microwave heating section which was called as MATS-CSM. The heating patterns of pre-packaged foods in the MATS system were correctly predicted by the MATS-CSM.

The objective of this study was to develop a computer simulation model for mobile metallic temperature sensors used in a continuous MATS system based on MATS-CSM. Performances of the mobile metallic sensors in a MATS system were investigated at different cold spot locations and in two different orientations. Experiment tests were carried out to validate simulation results in terms of heating patterns and temperature profiles of the food samples.

2. Material and methods

2.1. Physical model

A simulation model was developed based upon MTAS-CSM. Only the microwave heating section was simulated in MATS-CSM. This section contains four microwave heating cavities. Each cavity consists of a rectangular box and two identical horn shaped applicators on its top and bottom. Microwave energy is delivered to the applicators by a standard waveguide WR975, through which only TE10 mode is supported. The front and top views of a cavity are shown in Fig. 1. The electric field component is in y direction (Ey) and it propagates in z direction to the load box which is filled with water and packaged foods. The packages are transported in the positive x direction by a conveyor belt immersed in a thin bed (29 mm) of circulating hot water. Hot water is circulating in the opposite (negative x) direction to the moving packages at a speed of 40 L/min. The purpose of water immersion during microwave heating was to reduce edge over-heating in packaged foods. A detailed description of the MATS system and its operation are provided in (Resurrection et al., 2013).

The mobile metallic temperature sensor used in this study for experimental validation was the Tracksense Pro data logger. It consisted of two parts: a cylindrical base, and a long probe (Fig. 2). The length and the diameter of the base were 22 mm and 15 mm, respectively. A temperature sensor (PT 1000) was installed inside a protective metal tube 2 mm in diameter and 50 mm in length. The sensing element of the temperature sensor was 3 mm from the end of tube. Temperatures detected by the probe were stored in the cylindrical base in two seconds interval. The entire surface of this temperature sensor was made of metallic materials.

The size of the food samples used in this study was $135 \times 95 \times 16\ mm^3$. The mobile metallic sensor was imbedded in a packaged food sample. The sensor was placed in different directions to investigate the behavior of diffracted EM field components. The 2-D views of the food samples and the temperature sensors with two different placement orientations are illustrated in Fig. 3. Alternating electric field with Ey component was the source to heat foods. Magnetic field component was not illustrated since it has no effect on food materials. The placement orientation of a metallic sensor was explained by an orientation angle while keeping the probe end at the same location. The angle $(\varphi, 0^\circ \leqslant \varphi \leqslant 90^\circ)$

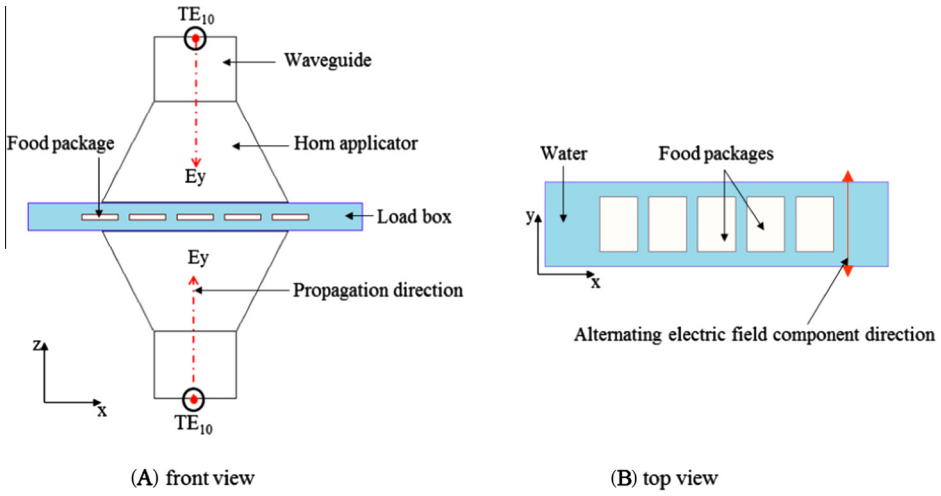

Fig. 1. Schematic of a microwave heating cavity: (A) front view, (B) top view. The component of the alternating electric field is in *y* direction (Ey) and it propagates in *z* direction.

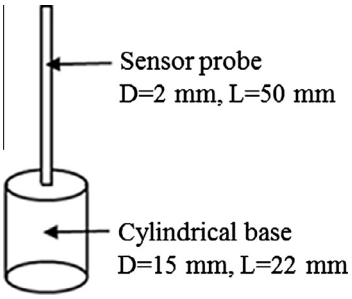

Fig. 2. Schematic of the metallic temperature sensor. The diameter (D) and length (L) for the sensor probe and base are 2 mm, 50 mm and 15 mm, 22 mm, respectively.

between the direction of a metallic temperature sensor (along the probe length direction) and the direction of alternating electric field component was called the orientation angle. The orientation angle was defined as 0° (Fig. 3A1) and 90° (Fig. 3B1) respectively, when the sensor was parallel or perpendicular to the electric field component.

2.2. Governing equations for EM field and heat diffusion

A microwave heating process includes two thermal phenomena: microwave heating due to EM field propagation and heat diffusion within foods. The fundamental theory for microwave propagation is based on Maxwell's equations. In this study, EM waves were calculated through the conformal FDTD method based on the integral form of Maxwell's equations (Balanis, 1989).

$$\oint_c \vec{E} \cdot \vec{dl} = -\frac{\partial}{\partial t} \oint_s \vec{B} \cdot \vec{ds} \tag{1}$$

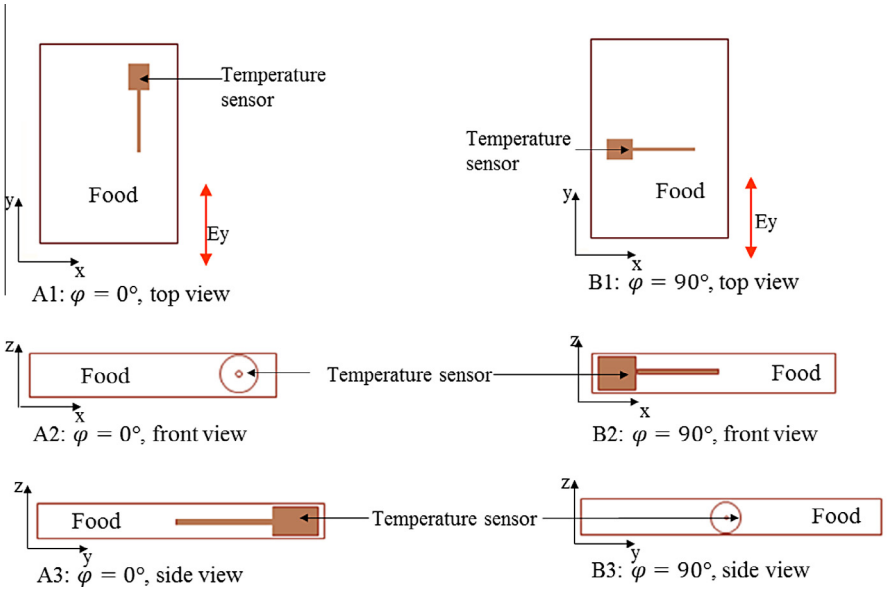

Fig. 3. Placement orientations for the temperature sensors within foods in different views: (A1) $\varphi = 0°$, top view, (A2) $\varphi = 0°$, front view, (A3) $\varphi = 0°$, side view, (B1) $\varphi = 90°$, top view, (B2) $\varphi = 90°$, front view, (B3) $\varphi = 90°$, side view. The orientation angle ($\varphi, 0^\circ \leqslant \varphi \leqslant 90^\circ$) is the angle between the direction of a metallic temperature sensor (along the probe length direction) and the direction of electric field component. Alternating electric fields were distributed in food with a component of Ey.

$$\oint_c \vec{H}\cdot\vec{dl} = -\frac{\partial}{\partial t}\oiint_s \vec{D}\cdot\vec{ds} + \oiint_s(\vec{j}_i+\vec{j}_c)\vec{ds} \quad (2)$$

$$\oiint_s \vec{D}\cdot\vec{ds} = Q^e \quad (3)$$

$$\oiint_s \vec{B}\cdot\vec{ds} = 0 \quad (4)$$

where $\vec{E}$ is electric field intensity, $\vec{D}=\varepsilon\vec{E}$ is electric flux density, $\vec{H}$ is magnetic field intensity, $\vec{B}=\mu\vec{H}$ is magnetic flux density. $\vec{j}_i$ is the impressed (source) electric current density and $\vec{j}_c$ is the conduction electric current density. Q^e is the electric charges in the volume enclosed by surface S. ε and μ are the permittivity and permeability of the media that EM waves propagate in. In free space, the value of permittivity is $\varepsilon_0 = 10^{-9}/36\pi$ F/m and the permeability is $\mu_0 = 4\pi\times10^{-7}$ H/m.

Conduction heat transfer takes place inside foods due to uneven temperature distribution and convection heat transfer exists between food and the hot water. The equation for conduction heat transfer is (Rakesh et al., 2010):

$$\nabla(K(T)\cdot\nabla T) + P = \rho C_p(T)\frac{\partial T}{\partial t} \quad (5)$$

The equation for convection heat transfer between food and circulating water is:

$$q = hA(T_W - T) \quad (6)$$

$K(T)$ is the thermal conductivity of food and $C_p(T)$ is the specific heat. Both are functions of temperature (T). ρ is the density of food. q and h are the energy exchange and the heat transfer coefficient between foods and water, respectively, A is the interface area. T_W is the temperature of hot water and T is the temperature of food.

In Eq. (5), P stands for the dissipated power of microwave in a certain volume:

$$P = 2\pi f\varepsilon_0\varepsilon_r''|E|^2 \quad (7)$$

In which, f is microwave frequency, ε_r'' is the relative dielectric loss factor of dielectric material. E is the instantaneous electric field vector, $E = E(x, y, z; t)$.

2.3. Development of the numerical models

A commercial EM field solver QuickWave 3D version 7.5 (QW3D, Warsaw, Poland) was used to solve the integral form of Maxwell's equation. Furthermore, an attached Basic Heating Module of QuickWave (QW-BHM) provides FDTD calculation for heat transfer. The QW-BHM allows adjustment of dielectric and thermal properties of media according to changing temperature, which can perform simulations that are more approximate to the actual microwave process. It also supports load rotation and movement in horizontal direction for simulating moving samples. Furthermore, the newly released module of QW3D provides a support for the movement of metal elements which can be used to simulate the mobile metallic temperature sensor in a MATS system.

Temperature dependent dielectric and thermal properties of the simulated foods were saved in a separate file which could be recognized by QW-BHM. The initial temperature of food was set as uniform (72 °C) to simulate the food packages processed by the preheating section of the MATS system. Water temperature was set as a constant of 125 °C to simulate the high speed circulating condition. All water properties were treated as constant.

The microwave heating section in the MATS system had two open ends in x direction which was connected with preheating and holding section. A perfect electric conductor (PEC) boundary condition was recommended for the numerical terminations at these two ends (Chen et al., 2007). The PEC boundary condition was also applied at the two open ends in this study. Besides, a 300 mm long load box filled with water was applied to each open end of the section to attenuate the intensity of EM field propagating to the PEC ends. The metallic temperature sensor was assumed as PEC to simulate its high conductivity ($\sim10^{-6}$ S/m). In the QW-BHM, adiabatic conditions were applied at the boundaries between PEC and dielectric materials (foods, water). QW-BHM automatically assumes that there is no heat exchange between PEC and other materials. As a result, the PEC had no temperature evolution through the simulation process. A constant temperature of a PEC was initially set up at the beginning of the simulation. The temperature of the metallic temperature sensor was set as 121.1 °C which is the objective temperature in sterilization. Convection heat diffusion occurred at the surface between hot water and the packaged food, the heat transfer coefficient was set as 180 $Wm^{-2}K^{-1}$. It was chosen based the agreement between simulation results and experiment results for hot water heating (Resurrection, 2012).

The general size of the FDTD cells occupied by the food sample was the same as the one in MTAS-CSM which had a size of $4\times4\times1$ mm^3 (Resurrection, 2012). However, in this study, the size of the cells in the probe vicinity of the metallic sensor was refined. The sizes of the FDTD cells at the probe end of the temperature sensor are shown in Fig. 4. In the top view (x–y plane), if $\varphi = 90°$, the cell size was 3×3 mm^2 around the probe end, and a 3×2 mm^2 cell was modified to keep the probe occupying a whole cell since its diameter was 2 mm. If $\varphi = 0°$ the cells occupied by the probe were modified to 2×3 mm^2 and other cells were kept as 3×3 mm^2. In the thickness direction (z–x or z–y plane), a finer mesh was defined. The cell occupied by the sensor probe had a size of 3×0.5 mm^2 and the around ones were 3×1 mm^2. That is, the cell size in the probe of a metallic temperature sensor was either $3\times2\times0.5$ mm^3 or $2\times3\times0.5$ mm^3 depending on its directions and the cell size in the adjacent food was $3\times3\times1$ mm^3. The same FDTD cell sizes were applied in the simulation models without a metallic sensor to make comparison.

The power setting for the four microwave heating cavities in the MATS system were based upon previous experience and were set to 6.0, 4.7, 2.8 and 2.7 kW, respectively. Thirty-two discrete moving steps were applied to simulate the continuous moving process. As was done in the case of the traveling distance, the total heating time was discretized and averagely distributed into these steps. Sensitivity studies were performed for smaller cell sizes and larger number of moving steps. Results indicated that the simulation models were robust and displayed convergence. Based on the balance between simulation accuracy and time consumption current cell size and moving steps were chosen.

2.4. Experimental validation

Experimental tests were carried out through the MATS system to validate the simulation models. Preformed whey protein gel (WPG) was used as model food to provide a homogeneous sample (Lau et al., 2003; Wang et al., 2009). The WPGs were made by mixing 75.4% water, 23.3% protein, 0.3% salt and 1% D-ribose. The uniform mixture was placed into containers and cooked in an 80 °C water bath for 40 min. After cooking, the solidified gels were stored at 4 °C refrigerator for at least 24 h before the MATS process.

The probe end of a temperature sensor was located within WPG at a cold spot area predetermined by the computer simulation method. Packaged with Alfredo sauce, a total weight of 215 g sample was sealed in a pouch which is transparent to microwave. The packaged WPG with temperature sensor was placed in the conveyor belt and transported through the MATS system. To eliminate the interference from adjacent sensors, at least two packages without sensors were placed between each package with a sensor. The moving speed of the conveyor belt during microwave heating

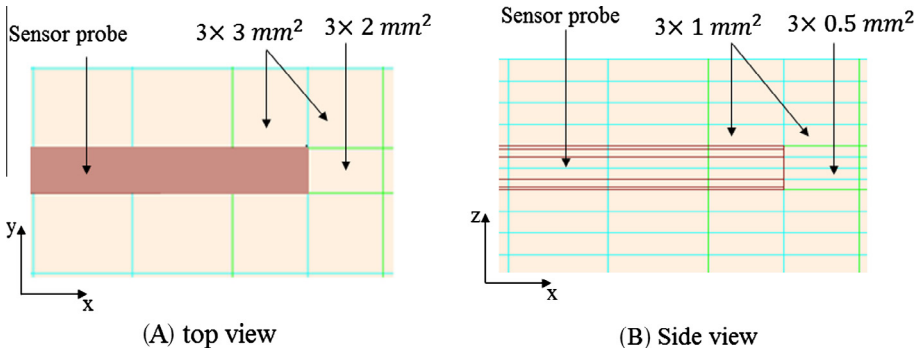

Fig. 4. FDTD cell sizes at the probe end of a metallic temperature sensor.

section was 18 mm/s resulting in a final heating time of 170 s. The processed samples were taken out at the end of the cooling section and then analyzed for heating pattern.

3. Results and discussion

3.1. Heating pattern generated from simulation model without sensor

The heating pattern obtained from computer simulation was generated from the temperature distribution in each FDTD cell. By setting different colors to represent different temperature levels, a heating pattern image was obtained. Temperature distribution in the middle layer in *x*-*y* plane can best represent the heating pattern of an our concern where it received the least influence by hot water heating. The cold spots should be located in this layer due to lowest microwave energy density. Each heating pattern generated from a simulation model shown in this study was a top view (*x*–*y* plane) of the temperature distribution in the middle layer. The heating pattern without sensor is shown in Fig. 5. A symmetric temperature distribution (in either *x* or *y* direction) is shown in the heating pattern. There are two hot spot and three cold spot bands interlaced in *y* direction except for the edge heating. Six cold spots (cold spot A1, A2, A3, A4, B1 and B2) and two local hot spots (hot spot A and B) located in these bands vicinities. Based upon the symmetrical characteristic, cold spots A1–A4 should have similar heating rate, same statement can be made for cold spot B1 and B2. Cold spots A2 and B2 were used to represent these two different cold spots and the metallic temperature sensors placed at these locations were simulated.

3.2. Heating patterns and temperature profiles influenced by the metallic sensors

In the simulation models, temperature sensors were placed at cold spots A2 and B2 (Fig. 5) with two orientation angles ($\varphi = 0°$ or 90°) to study the influences on the heating patterns and temperature profiles. Top view heating patterns of these simulation models are demonstrated in Fig. 6. Compared with the heating pattern without sensor in Fig. 5, the global distributions of cold and hot spots were not affected by the existence of the temperature sensors. However, there were some minor shifts in local temperature distribution. In Fig. 6A and C, relative higher temperatures appeared close to the temperature sensor. These local variations were more apparent in hot spot areas than in cold spot areas. This is because the metallic temperature sensors cut off the continuous electric field component in the *y* direction. The electric field intensity in the interrupted domain caused an increase in the local temperatures. These increases were more obvious adjacent to the hot spot areas. In Fig. 6B and D, higher electric field intensity caused by the based parts of metallic sensors changed the local heating patterns.

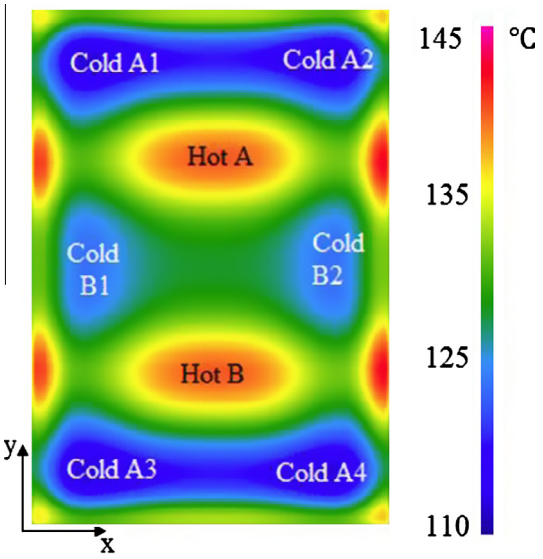

Fig. 5. Heating pattern generated from the computer simulation model without the temperature sensor.

The distortion in temperature distribution due to presence of the metallic temperature sensor was intensified at higher electric field intensity and by larger metallic volume. Similar distortion at the edge of a PEC and singularities at sharp tips have been reported by Meixner (1972).

To evaluate the accuracy of temperatures detected by the metallic temperature sensors, temperature profiles at cold spot locations were extracted from simulation results. The 32 simulation steps in each model can provide 32 elements for the temperature profile. Each element was obtained by averaging the temperatures at the probe end vicinity. Since the sensing element of the temperature sensor is 3 mm from the probe end, all the FDTD cells within 3 mm from the probe end were used to obtain the average temperatures. To avoid size difference among FDTD cells, the volume-temperature average was conducted by:

$$T_{av} = \frac{\sum_{i=1}^{n}(T_i V_i)}{\sum_{i=1}^{n} V_i} \tag{8}$$

where T_{av} is the averaged temperature, T_i is the temperature in a FDTD cell and V_i is the cell volume. The result of a temperature profile for the simulation model without the metallic temperature sensor was extracted from the same FDTD cells to make comparison. The temperature profiles influenced by the sensor conditions (without sensor, $\varphi = 0°$ or 90°) at cold spot A2 and B2 are shown in Fig. 7.

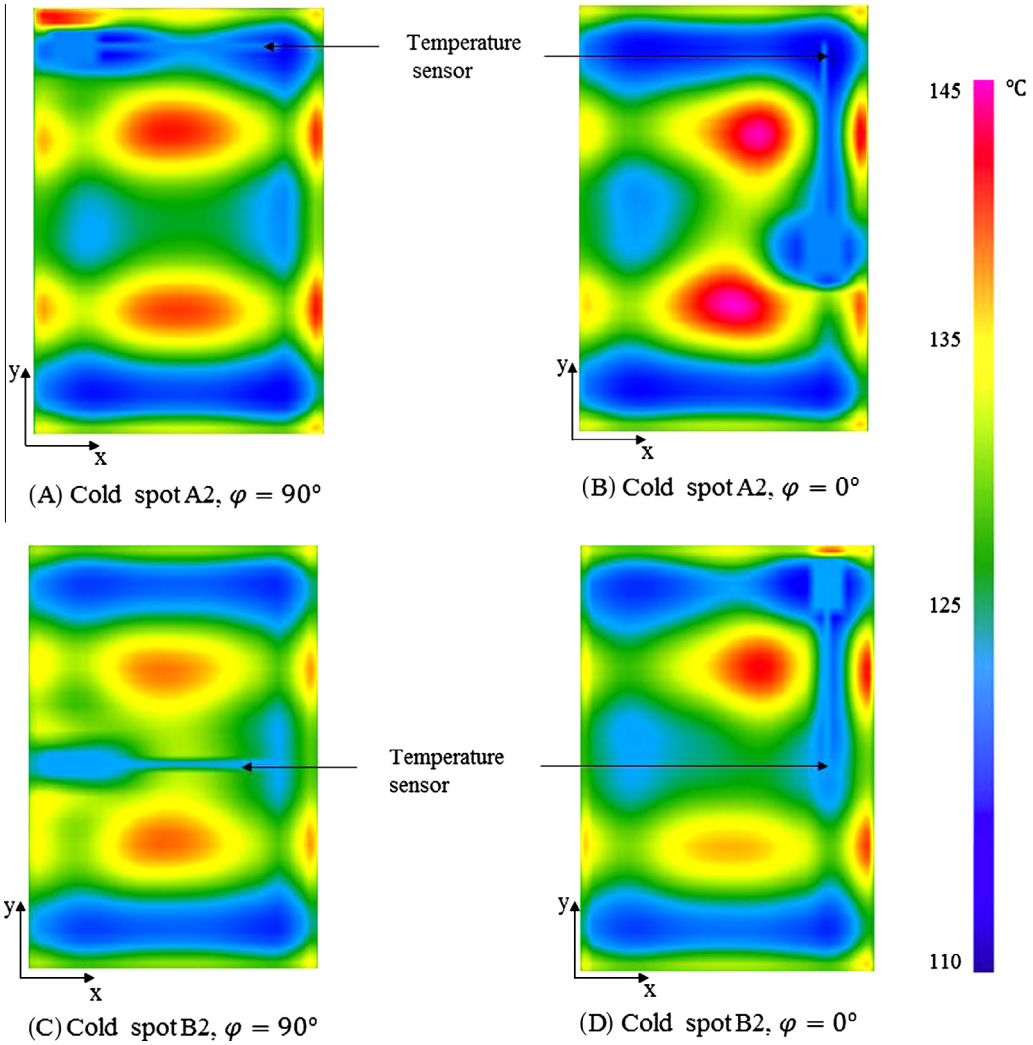

Fig. 6. Heating patterns generated from the computer simulation models with the metallic temperature sensors. The sensors in different simulation models either had a different location or a different orientation angle: (A) $\varphi = 90°$ at cold spot A2, (B) $\varphi = 0°$ at cold spot A2, (C) $\varphi = 90°$, at cold spot B2, (D) $\varphi = 0°$ at cold spot B2.

In Fig. 7, temperature profiles at the cold spot A2 were similar to the profiles at cold spot B2 in general trends. Good agreement in temperature profiles was observed between the one without sensor and the one with a sensor in the orientation of $\varphi = 90°$. The results implied that when placing sensors with $\varphi = 90°$, the metallic mobile temperature sensor had little influence on the measured temperature profiles. However, fluctuating temperature profiles were obtained when foods are traveling through each microwave heating cavity and the sensors were placed in an orientation angle of $\varphi = 0°$. These fluctuations were unexpected since the temperature at a cold spot should not decrease due to the heat diffusion from adjacent domain. The presence of fluctuations in a temperature profile implied that a local hot spot occurred in the tip area of the sensor with $\varphi = 0°$, caused by an electric field singularity.

The dissipated microwave power density within a food containing a metallic temperature sensor with $\varphi = 0°$ is shown in Fig. 8 to reveal the field singularity. For illustrations, three snapshots of the power density were taken at the entrance, center and exit of cavity 2. Higher microwave power density implies stronger electric field intensity. The electric field intensity at the tip of the metallic sensor reached its maximum while the food moved to the center position of the cavity. When traveling through the whole length of this cavity, the electric field intensity at the sensor tip increased from the entrance to the center position and then decreased from the center to the exit position.

In general, when the temperature sensor was entering into a microwave heating cavity with $\varphi = 0°$, the electric field singularity and local overheating were enhanced by the increasing electric field intensity as reflected by a sharp temperature increase in the temperature profile. The singularity and local overheating reached maximum when the temperature sensor moved to the center of a microwave heating cavity. When the temperature sensor was leaving the microwave heating cavity, the singularity decreased with reducing electric field intensity and lowered the level of local overheating. Due to heat transfer, the energy in the local overheating region will flow to the vicinity region causing temperature reading to decrease between the center positions of two adjacent cavities. The fluctuations were dramatic in the first two cavities compared with the last two cavities because that the powers in the first two cavities (6.0 and 4.7 kW) were higher than the other two (2.8 and 2.7 kW). In this study, the good agreement between the temperature profile without sensor and the one with $\varphi = 90°$ indicated that the local overheating can be reduced to minimum by orientating the metallic temperature sensor perpendicular to the electric field component.

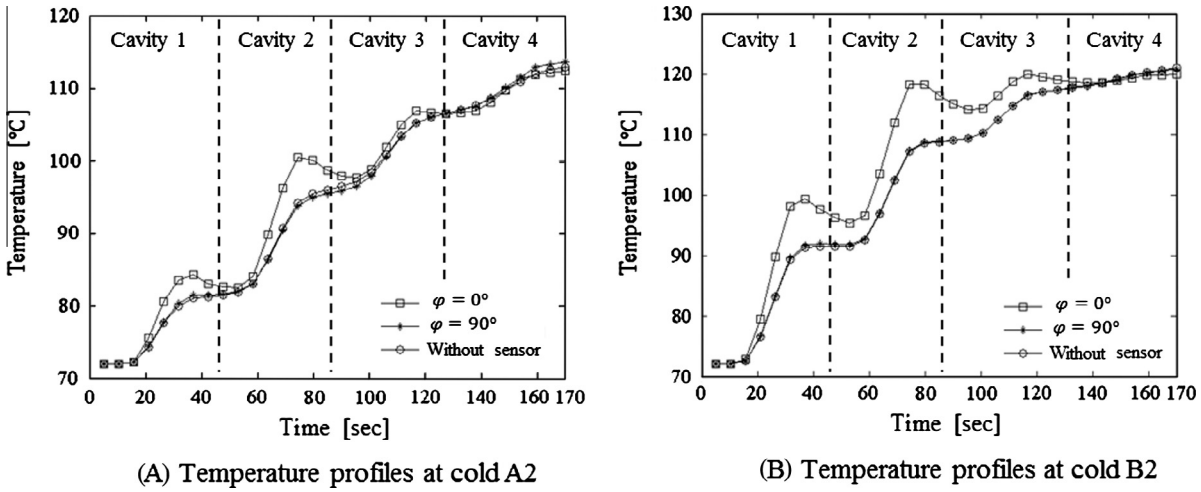

Fig. 7. Comparison of temperature profiles for different metallic temperature sensor conditions within foods: $\varphi = 0°$ (└▫─), $\varphi = 90°$ (└┼─) and without sensor (└●─). The temperature profiles were obtained from different computer simulation models at cold spot A2 (A) and cold spot B2 (B).

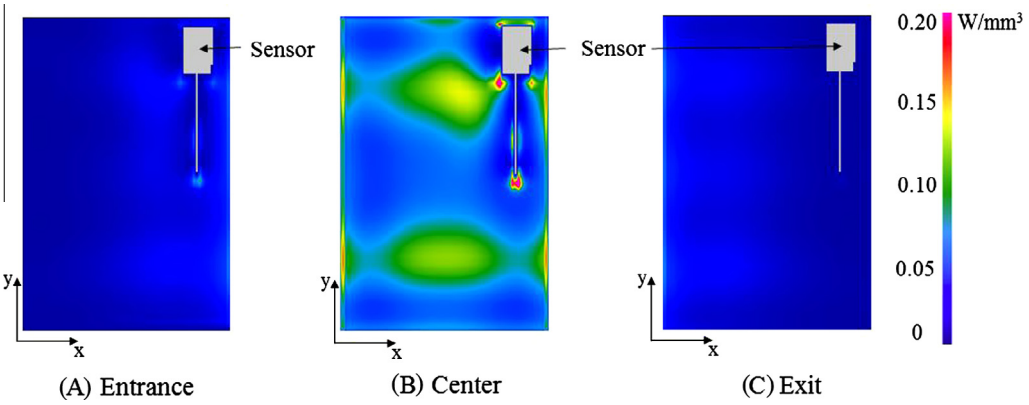

Fig. 8. Microwave power dissipation within food packages (top view) at different positions of Cavity 2: (A) at the entrance of cavity 2, (B) at the center of cavity 2, (C) at the exit of Cavity 2.

3.3. Experimental validation

The cold spot B2 was chosen to carry out experimental validation. B2 had a higher final temperature than cold spot A2 (Fig. 7). Probe ends of the sensors were placed at cold spot B2 in two orientations ($\varphi = 0°$ or 90°) and each was packaged with separated WPG samples (Fig. 3). At the end of the experiment, the heating pattern of the WPG was obtained through computer vision method and the temperature profile was retrieved from the temperature sensor. The heating patterns are shown in Fig. 9. Similar to heating patterns obtained from simulation results (Figs. 5 and 6C and D), there are three cold spot areas and two hot spot areas alternately distributed in y direction except for edge heating. The influences caused by metallic temperature sensors on heating patterns were the same as simulation results.

Besides the heating pattern, temperature profiles recorded by the metallic temperature sensors and the related simulation results are shown in Fig. 10. The variations of temperature in experimental results among replications were caused by possible differences in the tip locations of the temperature sensors. Differences among the tip locations may occurred when the sensors were placed into foods by hand. However, the differences of tip locations can only affect the magnitude of the collected temperature. They caused no changes in the general trend of the temperature profiles. The general trend of the temperature profiles between experiment and simulation results are the same.

The fluctuant temperature profile was verified by the metallic temperature sensor in experiment tests with $\varphi = 0°$. The fluctuations were observed in every microwave heating cavity (Fig. 10B) and they are more noticeable in the first two cavities. The unexpected fluctuations were removed by orienting the metallic temperature sensor to $\varphi = 90°$ (Fig. 10A). Results verified that overheating appeared at the tip of a metallic temperature sensor when the sensor was placed in y direction (u = 0°). The local overheating was caused by electric field singularity and it could be enhanced by higher microwave power which delivered higher electric field intensity. This field singularity could be avoided by placing the probe perpendicular to the electric field component. The difference in the tip location of the metallic temperature sensor would not influence the general trend of the temperature profile.

The temperature profiles in simulation results did not completely coincide with the experimental results especially in the last two cavities. Many parameters in simulation models may lead to the difference, such as the heat transfer coefficient between food and hot water, the dielectric and thermal properties of model foods and ideal assumption of the PEC metallic temperature sensor. Overall, simulation models provided results in general agreements with experimental results in terms of heating patterns and temperature profiles. In particular, the trends of the temperature profiles influenced by the metallic temperature sensors were well confirmed by experimental tests.

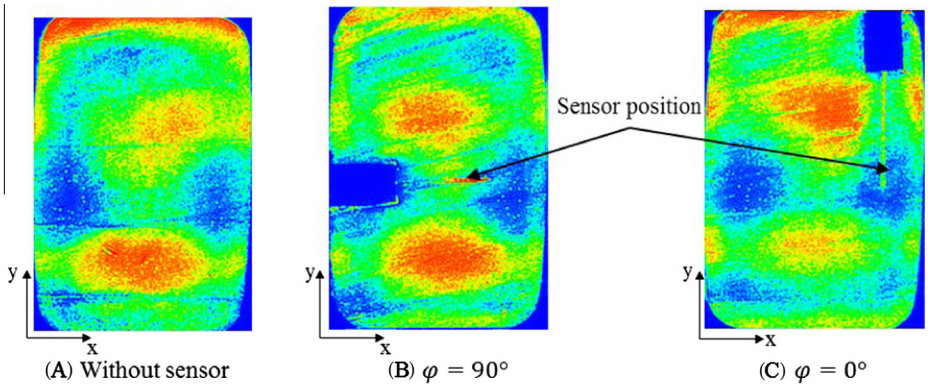

Fig. 9. Heating patterns obtained from experimental results with different sensor conditions at cold spot B2: (A) without sensor, (B) $\varphi = 90°$, (C) $\varphi = 0°$. Various colors stand for different temperature levels. Temperatures increase in order with colors changing from blue, green, yellow to red. (For interpretation of the references to colour in this figure legend, the reader is referred to the web version of this article.)

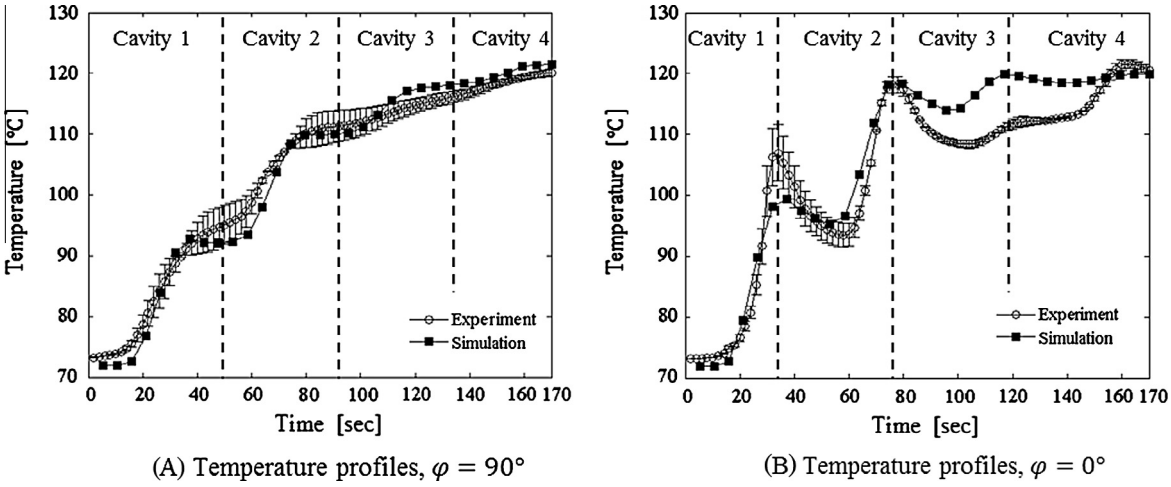

Fig. 10. Comparison of temperature profiles for experimental (└-) and simulation (└-) results at cold spot B2 with different orientation angles of the temperature sensor: (A) $\varphi = 90°$, (B) $\varphi = 0°$.

4. Conclusion

Mobile metallic temperature sensors showed no influence on the general heating pattern of a packaged model food in MATS system. However, there was a temperature increase close to the sensor which caused a local modification of heat pattern once the sensor cut off the electric field component. This distorted heating pattern was noticeable at the domain close to a hot spot area and base part of the sensor. The local temperature increase was attributed to the local overheating that caused by an electric field distortion or singularity. The level of the field singularity and local overheating can be enhanced by higher electric field intensity and larger metallic volume. If a field singularity occurred at the tip of the metallic temperature sensor, the temperature profile displayed fluctuations with varying electric field intensity in continuous MATS system. A metallic temperature sensor with a small volume is recommended to reduce its influence on the heating pattern. To remove the influence of field singularities on the temperature profile, the metallic temperature sensor should be placed perpendicular to the electric field component. In conclusion, the mobile metallic temperature sensor can be used in a microwave heating system while a right placement orientation was arranged to obtain a reliable temperature profile.

Further studies are needed to understand the field singularities and local overheating affected by high microwave power used in industrial applications and to understand the influences on food safety and quality. This will support the application of the mobile metallic temperature sensors in commercial microwave heating system.

Acknowledgements

This project was supported by the Agriculture and Food Research Initiative of the USDA National Institute of Food and Agriculture, grant number #2011-68003-20096. The authors also thank the Chinese Scholarship Council for providing a scholarship to Donglei Luan for his Ph.D. studies at WSU.

References

Balanis, C.A., 1989. Advanced Engineering Electromagnetics. John Wiley, New York.
Bladel, J.V., 1985. Field singularities at metal-dielectric wedges. IEEE Transactions of Antennas and Propagation 33 (4), 450–455.
Bouwkamp, C.J., 1946. A note on singularities occurring at sharp edges in electromagnetic diffraction theory. Physica 12 (7), 467–475.
Chan, C.T., Reader, H.C., 2000. Understanding Microwave Heating Cavities. Artech House Inc., Norwood, MA.
Chen, H., Tang, J., Liu, F., 2007. Coupled Simulation of an electromagnetic heating process using the finite difference time domain method. Journal of Microwave Power & Electromagnetic Energy 41 (3), 50–68.

Chen, H., Tang, J., Liu, F., 2008. Simulation model for moving food packages in microwave heating processes using conformal FDTD method. Journal of Food Engineering 88, 294–305.

Datta, A.K., Berek, H., Little, D.A., Ramaswamy, H.S., 2001. Measurement and Instrumentation. In: Datta., A.K., Anantheswaran, R.C. (Eds.), Handbook of Microwave Technology for Food Applications. CRC press, Boca Raton, FL., pp. 279–296.

Dev, S.R.S., Gariepy, Y., Orsat, V., Raghavan, G.S.V., 2010. FDTD modeling and simulation of microwave heating of in-shell eggs. Progress in Electromagnetic Research M 13, 229–243.

Egorov, S.V., Eremeev, A.G., Plotnikov, I.V., Sorokin, A.A., Xharova, N.A., Bykov, Y.V., 2006. Edge effect in microwave heating of conductive plates. Journal of Institute of Physics D: Applied Physics 39, 3036–3041.

Guan, D., Plotka, V.C.F., Clark, S., Tang, J., 2002. Sensory evaluation of microwave treated macaroni and cheese. Journal of Food Processing & Preservation 26 (5), 307–322.

Guan, D., Gray, P., Kang, D.H., Tang, J., Shafer, B., Ito, K., Younce, F., Yang, T.C.S., 2003. Microbiological validation of microwave-circulated water combination heating technology by inoculated pack studies. Journal of Food Science 68 (4), 1428–1432.

Holdsworth, S.D., 1985. Optimization of thermal processing. Journal of Food Engineering 4, 89–116.

Holland, R., 1993. Pitfalls of staircase meshing. IEEE Transactions on Electromagnetic Compatibility 35 (4), 434–439.

Kyuma, K., Tai, S., Sawada, T., Nunoshita, M., 1982. Fiber-optic instrument for temperature measurement. IEEE Journal of Quantum Electronics 18 (4), 676–679.

Lau, M.H., Tang, J., Taub, I.A., Yang, T.C.S., Edwards, C.G., Mao, R., 2003. Kinetics of chemical marker formation in whey protein gel for studying microwave sterilization. Journal of Food Engineering 60, 397–405.

Meixner, J., 1972. The behavior of electromagnetic Fields at edges. IEEE Transactions on Antennas and Propagation 20 (4), 442–446.

Pandit, R.B., Tang, J., Mikhaylenko, G., Liu, F., 2006. Kinetics of chemical marker M-2 formation in mashed potato-a tool to locate cold spots under microwave sterilization. Journal of Food Engineering 76, 353–361.

Pandit, R.B., Tang, J., Liu, F., Pitts, M., 2007a. Development of a novel approach to determine heating pattern using computer vision and chemical marker (M-2) yield. Journal of Food Engineering 78, 522–528.

Pandit, R.B., Tang, J., Liu, F., Mikhaylenko, G., 2007b. A computer vision method to locate cold spots in foods in microwave sterilization process. Pattern Recognition 40, 3667–3676.

Rakesh, V., Seo, Y., Datta, A.K., McCarth, K.L., McCarth, M.J., 2010. Heat transfer during microwave combination heating: computational models and MRI experiments. American Institute of Chemical Engineers Journal 56 (9), 2468–2478.

Ramaswamy, H.S., Rauber, J.M., Raghavan, G.S.V., Van De Voort, F.R., 1998. Evaluation of shielded thermocouples for measuring temperature of foods in a microwave oven. Journal of Food Science and Technology 35 (4), 325–329.

Resurrection, F.P., 2012. Microwave Assisted Thermal Processing of Homogeneous and Heterogeneous Food Packaged in a Polymeric Container. PhD Dissertation: Washington State University, Biological System Engineering.

Resurrection, F.P., Tang, J., Pedrow, P., Cavalieri, R., Liu, F., Tang, Z., 2013. Development of a computer simulation model for processing food in a microwave assisted thermal sterilization (MATS) system. Journal of Food Engineering 118, 406–416.

Tang, J., Liu, F., Pathak, S., Eves, G., 2006. Apparatus and Method for Heating Objectives with Microwaves. U.S. Patent 7,119,313.

Van De Voort, F.R., Laureano, M., Smith, J.P., Raghavan, G.S.V., 1987. A practical thermocouple for temperature measurement in microwave ovens. Canadian Institute of Food Science and Technology Journal 20 (4), 279–284.

Wang, S., Tang, J., Younce, F., 2003. Temperature measurement. In: Dennis, R. (Ed.), Encyclopedia of Agricultural, Food, and Biological Engineering. Marcel Dekker, New York, pp. 987–993.

Wang, Y., Tang, J., Rasco, B., Wang, S., Alshami, A.A., Kong, F., 2009. Using whey protein gel as a model food to study the dielectric heating properties of salmon (Oncorhynchus gorbuscha) fillets. LWT – Food Science and Technology 42, 1174–1178.

Watanabe, S., Karakawa, M., Hashimoto, O., 2010. Computer simulation of temperature distribution of frozen material heated in a microwave oven. IEEE Transactions on Microwave Theory and Techniques 58 (5), 1196–1204.